Simulation of Detonation Initiation in Multifocused Systems

Lopato A.[1], Utkin P.[1,*], Vasil'ev A.[2]

[1] *Institute for Computer Aided Design RAS, Moscow, Russia*
[2] *Lavrentyev Institute of Hydrodynamics SB RAS, Novosibirsk, Russia*
**Corresponding author's email: pavel_utk@mail.ru*

ABSTRACT

The paper is devoted to the numerical modeling of detonation initiation in the "multifocused" system – the plane channel with the profiled end-wall. Two types of profiles are considered, namely one semi-elliptical reflector and two semi-elliptical reflectors connected by the part of plane wall. The channel is filled with the stoichiometric hydrogen-oxygen mixture. The range of incident shock wave Mach numbers, 2.5 – 2.8, is considered. Mathematical model is based on two-dimensional Euler equations supplemented by one-stage chemical kinetics model. The specific feature of the numerical algorithm of the second approximation order is the usage of fully unstructured computational grids with the triangular cells. The mechanisms of detonation initiation for all cases are described. It is shown that the end-wall profile in the form of two semi-elliptical reflectors connected by the part of plane wall reduces the time of shock-to-detonation transition in comparison with one reflector.

KEYWORDS: Detonation wave, initiation, multifocused system, numerical simulation, unstructured grids.

NOMENCLATURE

A	pre-exponential factor (kJ/mole)
p	pressure (Pa)
M	incident shock wave Mach number (-)
Q	heat release (MJ/kg)
R	universal gas constant (J/(mol·K))
T	temperature (K)
t	time (s)
u	x-component of gas velocity (m/s)
v	y-component of gas velocity (m/s)
x	abscissa of the Cartesian frame (m)
y	ordinate of the Cartesian frame (m)
Z	reactant mass fraction (-)

Greek

μ	molar mass (kg/mole)
ρ	density (kg/m^3)
γ	specific heat ratio (-)

Subscripts

k	computational cell number
vN	von Neumann parameters

Superscripts

n	time step number

INTRODUCTION

The problem of reactive mixture initiation is important as the interdisciplinary problem from the scientific, applied and ecological safety aspects points of view. The main goal is the determination of the critical conditions of initiation and its optimization due to the spatial distribution of the energy input and the time charactristics. Each mixture under given conditions (pressure, temperature, composition) is characterized by some specific spatial and time scales r_* and t_*. For

Proceedings of the Ninth International Seminar on Fire and Explosion Hazards (ISFEH9), pp. 247-256
Edited by Snegirev A., Liu N.A., Tamanini F., Bradley D., Molkov V., and Chaumeix N.
Published by St. Petersburg Polytechnic University Press
ISBN: 978-5-7422-6496-5 DOI: 10.18720/spbpu/2/k19-34

example, this is the length of the induction or reaction zone and the corresponding induction and reaction times. At the same time, under the given conditions the reactive mixture takes from initiator during the finite time interval t_0 in the finite spatial area $V_0 = f(r)$ some energy E_v (the part η of the initially stored in the initiator energy E_0):

$$E_v = \int_0^{t_0}\int_0^{V_0} \varepsilon(t,V)\,dtdV = \eta E_0,$$

where $\varepsilon(t, V)$ is the function which describes the spatial-time low of the energy input, ν is the dimension of the problem (ν = 1, 2, 3 for the plane, cylindrical and spherical symmetry correspondingly).

The effect of combustion and detonation excitation usually has a "threshold" (yes – no) character for any initiator, see Fig. 1. In the idealized model of a strong explosion, the governing parameter for an inert medium, which determines blast wave propagation, is the explosion energy. By analogy, the minimum energy of the initiator that ensures 100% excitation of combustion or detonation is usually called the critical energy of combustible mixtures, as well. The critical ignition energy E_{flame} (at least, in the case of spark ignition) is traditionally considered as the basic parameter of the fire hazard of mixture. The critical energy of detonation initiation E_* by an ideal (in terms of spatial and temporal characteristics) detonation initiator serves as a measure of the detonation hazard of mixture: the smaller the value of E_*, the more hazardous the mixture.

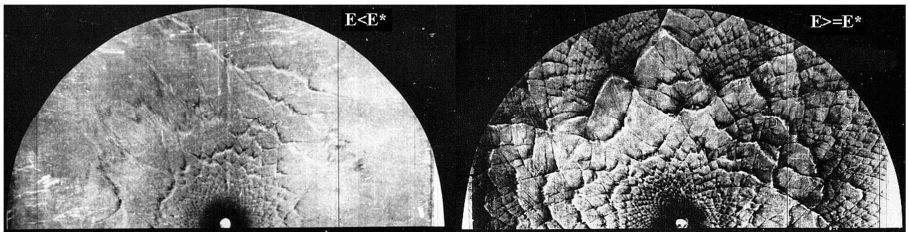

(a) detonation initiation failure (b) detonation initiation

Fig. 1. Smoked foil imprints of strong initiation for the initiator energy smaller than (a) and greater than (b) the critical energy of detonation initiation.

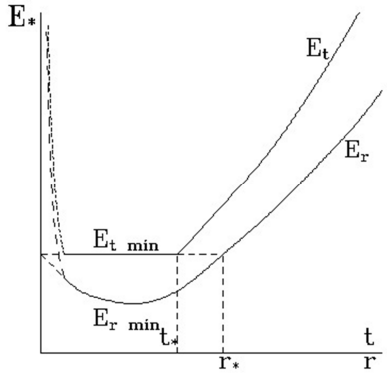

Fig. 2. Effect of the spatial and temporal components of the energy imparted by the initiator on the conditions of initiation of the combustible mixture.

It is known from the experiments on the variation of the energy input duration with the spatial size of the energy input domain being unchanged that the critical energy of initiation is the only criterial

parameter of the mixture, only if the initiating discharge duration does not exceed a certain critical value. Otherwise, the longer the discharge duration, the greater the energy required for detonation wave (DW) initiation, see Fig. 2. Each mixture at a fixed pressure is characterized by a certain temporal parameter t^0 such that the energy required for initiation E_t = const $\approx E_{\min}$ is taken as a critical energy of initiation E_* if the discharge duration is $t_0 \le t^0$. At $t_0 > t^0$ ("delayed" discharge), E_t is greater than $E_{\min}$ and increases with increasing t_0 (curve E_t in Fig. 2). It is found that upon the variation of the size and shape of the energy input domain, with the energy input being unchanged, the minimum critical energy can be significantly (by an order of magnitude or more) reduced as compared with the value determined by varying only the temporal characteristic of the input energy (curve E_r in Fig. 2).

Among different initiators (electric or laser spark, exploding wire, HE charge, thermal igniter, flux of hot and active particles etc.) the shock wave (SW) has the special role. The SW is able to compress and heat rapidly and uniformly the reactive mixture under the high pressure and temperature. The technique of SW is actively used for ignition delay time measurements. But even under the condition of uniform parameters of the mixture behind the SW the ignition occurs spontaneously at the separate points. In reactive mixtures where the instability development is typical the fact of ignition is determined, not by the average temperature, but by the "hot spot" temperature. Such "hot spots" can be created with the use of boundary conditions, for example due to the interaction of SW with obstacles, curved walls, periodical structures etc. Due to such non-one-dimensional SW patterns it is possible to create "hot spots" and noticeably reduce the critical energy (in comparison with one-dimensional models).

Many researchers have investigated the problem of gaseous detonation initiation as a result of relatively weak SW interaction with the profiled end-wall of the channel. In the experimental study [1] the reflectors in the form of two-dimensional (2D) wedges, semi-cylinder and parabola were considered. The peculiarities of mild and strong ignition inside the reflector cavity were visualized. It was shown that the mild ignition inside the reflector cavity can lead to detonation initiation outside the cavity. In the recent paper [2], containing both numerical and experimental results, the reflector in the form of three-dimensional (3D) cone was considered. Several different flow scenarios were detected in reflection of shock waves all being dependent on incident SW intensity: reflecting of SW, with lagging behind the combustion zone, formation of DW in reflection and focusing, and intermediate transient regimes.

A system of reflectors was considered in [3] and named "multifocused system". The multifocused system follows the concept of minimization of detonation initiation energy due to the time-spatial factors that are due to the usage of spatially distributed initiators that ignite non-simultaneously. The concept was realized in different solutions. It was shown in numerical studies [4] that it is possible to initiate detonation with the use of several discharges with the total energy input less than the energy of direct initiation. In [5], DW was formed as a result of successive actions of the distributed ignition pulses on the passing relatively weak SW. The close idea was realized in [6] both numerically and experimentally, but without additional energy input due to the special regular parabolic profile of the channel walls.

Numerical research of problems of DW initiation and propagation in the computational domains of a complex shape is connected with a number of questions related to the construction of computational grids in such domains, construction of monotone in some sense schemes of high approximation order on the selected class of grids, and also of infrastructure problems with large amounts of poorly structured data, including visualization issues. Despite all the achievements in the field of multiprocessor computing, the numerical studies of problems of physical and chemical hydrodynamics with a volume exceeding 10^8 computational cells are at the limit of the capabilities of researchers, due to the factors listed above. In [4, 6] the structured grids and the classical first

approximation order scheme of S.K. Godunov [4] or its modification based on some interpolation schemes for the approximation order increase [6] are used. At the same time, in relation to gas dynamics problems of chemically inert media, the apparatus of high approximation order schemes on completely unstructured computational grids, including SW problems, has been developed, see the best known paper [7]. The analysis of publications about the usage of such approaches to the study of high speed flows with chemical reactions has resulted in several papers [8 – 11]. In [9, 10] the finite element approach is applied. The most probable reason is the fact that, although the integration of the gas dynamics equations is a key element of the computational algorithm for the simulation of high speed flows with chemical reactions, the presence of strongly nonlinear sources on the right-hand sides of the equations significantly reduces the possibilities of applying many numerical methods that successfully deal with the gas dynamics problems of inert media.

The goal of the work is the investigation of the mechanisms of the detonation initiation in the multifocused systems [3], using the numerical technology based on the fully unstructured computational grids [12].

STATEMENT OF THE PROBLEM

Consider the plane channel filled with the quiescent stoichiometric hydrogen-oxygen mixture under an initial pressure 0.04 atm and ~~the~~ temperature of 298 K. Two variants of the end-wall shapes are considered [3]. The first one is the semi-elliptical curve, with the semi-axis 5 mm and 3.5 mm, see Fig. 3(a) ("elliptical reflectors were fabricated by milling, with a milling cutter angle of 45°. The reflector diameter is 10 mm" [3]). The second one consists of two semi-elliptical curves connected with the part of plane wall with the length 10 mm, see Fig. 3(b). The height of the channel for the first variant is 10 mm, for the second one – 20 mm. The length of the channels is 57.1 mm.

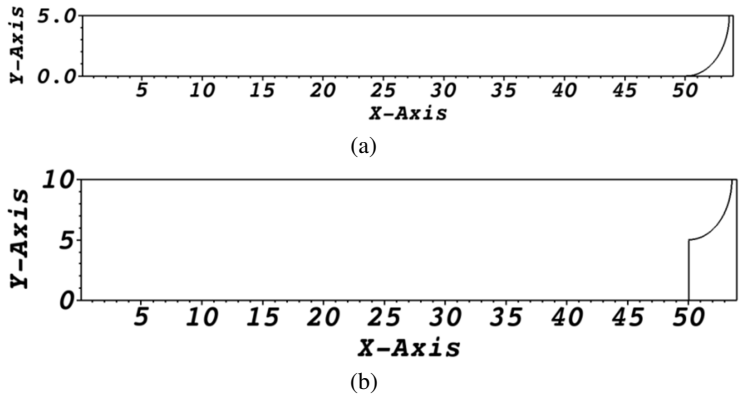

Fig. 3. Schematic statement of the problem. All sizes are in millimeters.

The incident SW location is x = 48 mm. The SW Mach numbers M = 2.5, 2.6, 2.7 and 2.8 are considered. At the initial instant of time in the area $x \leq 48$ mm the parameters behind the SW are set.

Slip-conditions are set at the bottom right boundaries, the inflow conditions at the left boundary, and the symmetry conditions at the upper boundary. The simulations last up to the moment of DW arrival at the left boundary. For the sake of computational cost, diminishing the computational domain corresponds to one half of the channel for the first variant and one fourth of the channel for the second variant.

Note that the semi-circular geometry of the reflector was investigated experimentally in [13]. For the same hydrogen-oxygen mixture and for the close range of incident the SW Mach number 2.2 – 2.8 the ignition delay times were measured for the case of a semi-circular reflector, and compared with the delays for the case of normal reflection of the SW.

MATHEMATICAL MODEL

The mathematical model is based on the 2D system of Euler equations, written in the Cartesian frame (x, y), supplemented by a one-stage chemical kinetics model:

$$\frac{\partial \mathbf{U}}{\partial t}+\frac{\partial \mathbf{F}}{\partial x}+\frac{\partial \mathbf{G}}{\partial y}=\mathbf{S}, \tag{1}$$

where

$$\mathbf{U}=\begin{bmatrix}\rho\\ \rho u\\ \rho v\\ e\\ \rho Z\end{bmatrix},\ \mathbf{F}=\begin{bmatrix}\rho u\\ \rho u^2+p\\ \rho uv\\ (e+p)u\\ \rho Zu\end{bmatrix},\ \mathbf{G}=\begin{bmatrix}\rho v\\ \rho vu\\ \rho v^2+p\\ (e+p)v\\ \rho Zv\end{bmatrix},\ \mathbf{S}=\begin{bmatrix}0\\ 0\\ 0\\ 0\\ \rho\omega\end{bmatrix},$$

$$e=\frac{\rho}{2}\left(u^2+v^2\right)+\rho\varepsilon,\ \varepsilon=\frac{p}{\rho(\gamma-1)}+ZQ,\ p=\frac{\rho}{\mu}RT,\ \omega=-A\rho Z\exp\left(-\frac{E}{RT}\right).$$

Here the notations are standard. The following parameters of the mixture are used: γ = 1.23, μ = 12 g/mol, Q = 7.37 MJ/kg, E = 76.2 kJ/mol, A = $9.16\cdot10^8$ m^3/(kg·s). The parameters γ (at the Chapman-Jouguet point), Q and E were taken from the database [14] (the case of a stoichiometric hydrogen-oxygen mixture under an initial pressure 0.2 atm; the pressure approximately corresponds to that behind the reflection from the planar wall SW, with the considered Mach numbers for the background pressure of 0.04 atm). Parameter A was calculated using the Konnov reaction mechanism reaction zone time τ:

$$A=\frac{1}{\tau\rho_{vN}}\exp\left(\frac{E}{RT_{vN}}\right),$$

where τ = 0.47 μs, ρ_{vN} = 0.541 kg/m^3, T_{vN} = 1682 K [14]. The "length of half-reaction" was verified in the Zeldovich-von Neumann-Doring solution, and was equal to 0.126 mm, while the given reaction zone length in [14] according to the Konnov reaction mechanism was equal to 0.24 mm. The differences in the results of calculations from tabulated values in [14] can be explained by the use of a constant value for the ratio of specific heats, γ, in the work.

The simulations for the first variant of the channel were carried out on the computational grid with the cells numbering about 790 000. For the second variant, the grid has about 1,450,000 cells. The maximum length of the side of the triangular cells for both grids was about 0.035 mm. So the resolution was about 4 cells per half reaction length. The grid convergence study for the channel with one semi-elliptical reflector, revealed that the usage of a twice more detailed computational grid did not lead to any changes in the main features of the detonation initiation mechanism. The main difference was that for the finer grid, the process occurred with a delay in time of several microseconds.

Of course, the detonation wave in gaseous mixtures in general has a 3D structure. However, the 2D simulations are widely used, see for example [4, 6, 9, 11], if the appropriate geometrical conditions are provided. The adequacy of the 2D simulations in the paper is conditioned by the geometry of the reflectors. In the experiments the channel had a rectangular cross section and the reflectors were fabricated to have the same 2D shape in the longitudinal cross-section. In general, the transition from the 2D to the 3D geometry leads to a decrease in the critical SW Mach numbers for the detonation initiation. For example, in [14] the fact is shown experimentally for the 2D wedge and 3D cone reflectors.

NUMERICAL ALGORITHM

The main feature of the computational technique is the use of completely unstructured computational grids, with triangular cells. A Delaunay triangulation is carried out to construct the grid.

The computational algorithm is based on the Strang splitting principle, in terms of physical processes [16]. When passing from one time layer to another, one first integrates the gas dynamics equations without considering the chemical reactions ($\mathbf{S} = 0$ in Eq. (1)), and thereby performs the first stage of the splitting procedure. In the second stage, the chemical reactions are taken into account, without considering the convection (the second stage of splitting).

The spatial part of Eq. (1) is discretized using the finite volume method:

$$\frac{\partial \mathbf{U}}{\partial t} \equiv \mathbf{L}(\mathbf{U}) = -\frac{1}{S_k}\sum_{\sigma=1}^{3}\left(\mathbf{F}_{k,\sigma} l_{k,\sigma}\right).$$

Here, the spatial index k corresponds to the number of calculated cell of area S_k. The summation is conducted over all edges σ of the cell k, $l_{k,\sigma}$ is the length of the edge with the index σ, $\mathbf{F}_{k,\sigma}$ is the vector of numerical flux through the edge in the direction of the unit normal $\mathbf{n}_{k,\sigma}$ that is external to the edge. To calculate the flux,

$$\mathbf{F}_{k,\sigma} = \mathbf{F}_{k,\sigma}\left(\mathbf{U}_k^n, \mathbf{U}_{k,\sigma}^n\right),$$

we pass from the initial global frame (x,y) to the local one, that is associated with the outer normal $\mathbf{n}_{k,\sigma}$ to the edge σ and the tangent vector $\boldsymbol{\tau}_{k,\sigma}$. Denoting the matrix of transformation as $\mathbf{T}_{\mathbf{n}_\sigma}$, the vector $\mathbf{U}_{k,\sigma}^n$ denotes the conservative variables vector in the triangular that has the common edge σ with the considered triangular k. The flux in the local frame is calculated using the AUSM scheme [17], extended for the case of a two-component mixture.

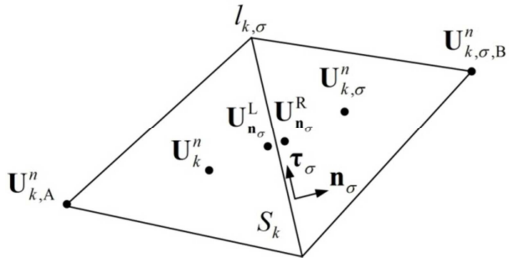

Fig. 4. To the reconstruction of grid functions.

For the approximation order increase, the following reconstruction of the grid functions is applied

[18]. The numerical flux in the local frame is computed using the following parameters from the left and the right sides of the edge σ (see Fig. 4):

$$\mathbf{U}^{\mathrm{L}}_{\mathbf{n}_\sigma} = \mathbf{T}_{\mathbf{n}_\sigma}\mathbf{U}^n_k + \frac{1}{2}\Psi\left(\mathbf{T}_{\mathbf{n}_\sigma}\mathbf{U}^n_k - \mathbf{T}_{\mathbf{n}_\sigma}\mathbf{U}^n_{k,\mathrm{A}}, \mathbf{T}_{\mathbf{n}_\sigma}\mathbf{U}^n_{k,\sigma} - \mathbf{T}_{\mathbf{n}_\sigma}\mathbf{U}^n_k\right),$$

$$\mathbf{U}^{\mathrm{R}}_{\mathbf{n}_\sigma} = \mathbf{T}_{\mathbf{n}_\sigma}\mathbf{U}^n_{k,\sigma} - \frac{1}{2}\Psi\left(\mathbf{T}_{\mathbf{n}_\sigma}\mathbf{U}^n_{k,\sigma} - \mathbf{T}_{\mathbf{n}_\sigma}\mathbf{U}^n_k, \mathbf{T}_{\mathbf{n}_\sigma}\mathbf{U}^n_{k,\sigma,\mathrm{B}} - \mathbf{T}_{\mathbf{n}_\sigma}\mathbf{U}^n_{k,\sigma}\right),$$

$$\mathbf{U}^n_{k,\mathrm{A}} = \frac{1}{|\mathrm{C_A}|}\sum_{i\in \mathrm{C_A}}\mathbf{U}^n_i,\ \mathbf{U}^n_{k,\sigma,\mathrm{B}} = \frac{1}{|\mathrm{C_B}|}\sum_{i\in \mathrm{C_B}}\mathbf{U}^n_i\ .$$

Here $\mathrm{C_A}$ denotes the set of triangles that have a common node, with the triangle k where the node is opposite to the edge σ. Similarly, $\mathrm{C_B}$ denotes the set of triangles that have a common node with the triangle k,σ where the node is opposite to the edge σ. The minmod limiter applied component-wise is considered as a limiter function Ψ:

$$\Psi(a,b) = \frac{1}{2}\mathrm{sign}(a+b)\min\left(|a|,|b|\right).$$

Time integration is carried out using the explicit Runge-Kutta method, of the second approximation order. The time step is chosen dynamically from the stability condition.

At the second stage of the algorithm, the system of ordinary differential equations of chemical kinetics for the Z variable and temperature in each computational cell of the grid is solved.

The estimation of the practical approximation order of the algorithm in the problem of isentropic vortex evolution [7] gave a value close to 2.

RESULTS OF SIMULATIONS

One semi-elliptical reflector

For the largest of the studied incident, SW Mach numbers 2.8, strong initiation occurs inside the reflector. After the primary focus of the flow on the axis of symmetry at the time of 6 μs, detonation is initiated in a few microseconds near the wall.

For M = 2.7 the initiation occurs at the boundary of the reflector ($x \approx 50$ mm). Fig. 5 illustrates the main stage of the process. At the time 5 μs the flow has not yet focused, one of the possible complex types of reflection of the incident SW from the elliptical wall is realized [18]. The snapshot at 10 μs shows the typical wave pattern in the reflector before the initiation. The wave R_1 is the part initially reflected from the elliptical wall wave. Waves R_2, R_3 and R_4 are formed after the reflection from the symmetry axis of the channel. At 13 μs wave R_4 traveling along the elliptical wall couples with R_1 and R_3 and enters the main channel. At the same time, as is seen from the isoline of Z, the autoignition has already occurred, with the subsequent pressure rise in the region near the symmetry axis of the channel. The pressure rise leads to the formation of the additional wave R_5. Detonation initiates at the time 15 μs, again as for the Mach number 2.8 near the wall of the channel after the wave R_5 amplifies the pressure in the region of collision of previous waves. At the next time period DW spreads in both directions, inside and outside the reflector. The pictures corresponding to the later moments of time show the multifront cellular, overdriven, DW propagating against the flow. To the beginning of the channel at a time of about 50 μs, the DW reaches the self-sustained regime. So for the Mach number 2.7 the mechanism of initiation is connected with the series of successive pressure waves propagated along the elliptical wall.

For M = 2.6 and 2.5, the process runs in a similar manner. The difference is that the local autoignition does not occur near the symmetry axis, and the waves R_i, i = 1 – 4, do not provide detonation initiation. Nevertheless, the initiation occurs approximately in the same region, close to the wall, not far from the reflector. For M = 2.5 the secondary initiation also takes place due to the multiple reflections in the planar part of the channel (the place of initiation is marked by black solid line in Fig. 6).

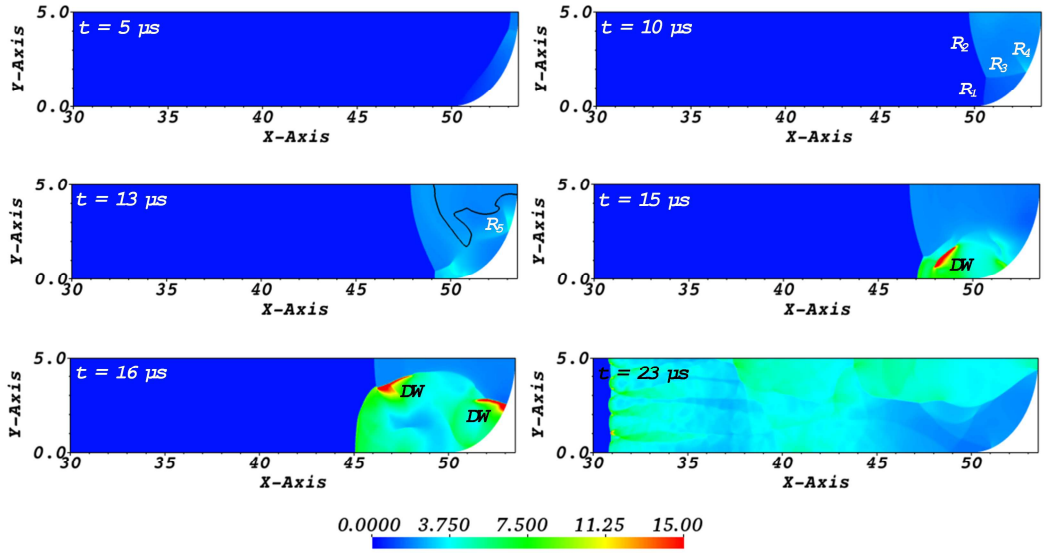

Fig. 5. Predicted pressure distributions at the successive time moments. One semi-elliptical reflector, M = 2.7. Axes are in millimeters. The scale is in atmospheres. The black line for the snapshot at t = 13 μs is the iso-line Z = 0.5.

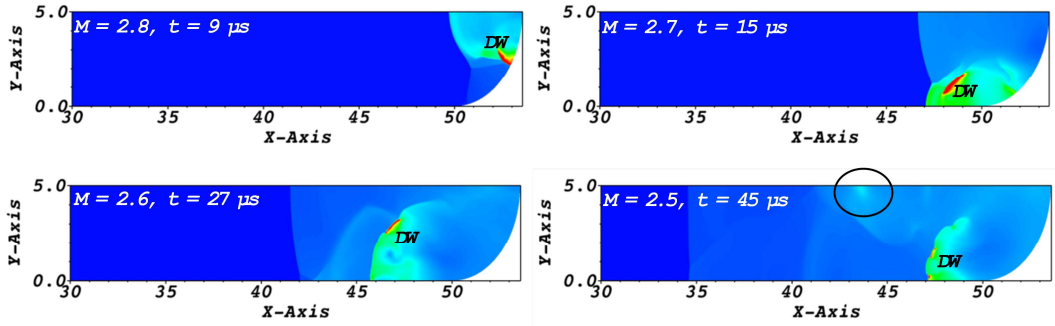

Fig. 6. Predicted pressure distributions at the moments of detonation initiation for different M. One semi-elliptical reflector. The scale is the same as in Fig. 5.

Fig. 6 summarizes the predicted pressure distributions at the moments of detonation initiation for the whole investigated incident SW Mach numbers range.

TWO SEMI-ELLIPTICAL REFLECTORS WITH THE PART OF PLANE WALL

The second type of reflector has an additional element to that considered above, namely the part of the plane wall. Consider the changes in the detonation initiation mechanism in this case. Fig. 7 corresponds to M = 2.7. The reflection of the incident SW from the planar wall provides an

additional wave, R_6, which diffracts and increases the pressure in front of the reflected waves in the reflector. More intensive combustion leads to the primary initiation near the symmetry axis of the channel at the time 12 μs. However, there is a detonation failure with the subsequent secondary initiation near the wall by a mechanism close to that described above for one reflector.

The positive effect of the wave R_6 leads to a small reduction of the shock-to-detonation time for M = 2.8, according to the mechanism for one reflector (see Fig. 8). For M = 2.6 the reduction is more noticeable. The initiation occurs both near the symmetry axis (primary) and near the wall (secondary).

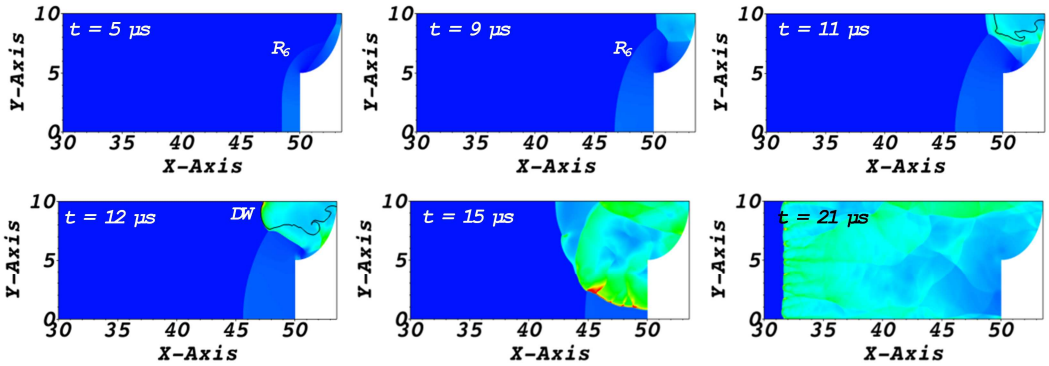

Fig. 7. Predicted pressure distributions at the successive time moments. Two semi-elliptical reflectors with the planar wall part, M = 2.7. Axis are in millimeters. The scale is the same as in Fig. 5. The black lines for the snapshots t = 11 μs and 12 μs are the isolines Z = 0.5.

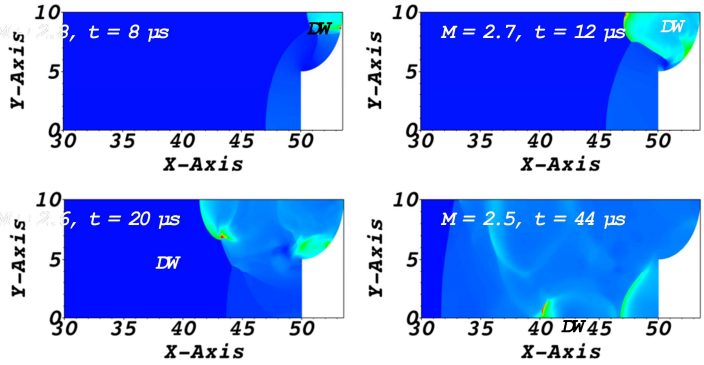

Fig. 8. Predicted pressure distributions at the moments of detonation initiation for different M. Two semi-elliptical reflectors with the planar wall part. The scale is the same as in Fig. 5.

CONCLUSIONS

The numerical simulation of detonation initiation due to the reflection of the incident shock with M = 2.5 – 2.8 from the profiled end-walls of the channel, filled with the stoichiometric hydrogen-oxygen mixture, is carried out. Two types of the reflectors are considered. The first one is the semi-elliptical reflector. The second comprises two semi-elliptical reflectors, with the additional plane part of the wall. Both geometries qualitatively correspond to those considered in the experimental study in [3]. For one semi-elliptical reflector the initiation always takes place near the wall inside the reflector. For high Mach numbers, the mechanism of initiation is connected with the series of successive pressure waves propagating along the elliptical wall or in the plane part (for low Mach numbers). For two semi-elliptical reflectors, with the part of plane wall ("multifocused system") the initiation for intermediate Mach numbers occurs in two places, namely near the symmetry axis, and

near the elliptical wall. The second type of the reflectors demonstrates the reduction of the shock-to-detonation time, due to the favorable effect of the additional wave reflected from the planar part of the wall, so the obtained results are in qualitative agreement with the experimental data of [3]. In [3], the critical Mach number of the incident shock wave for detonation wave initiation is lower for the second type of reflector.

The work was performed within the state task of ICAD RAS.

REFERENCES

[1] B.E. Gelfand, S.V. Khomik, A.M. Bartenev, S.P. Medvedev, H. Gronig, H. Olivier, Detonation and Deflagration Initiation at the Focusing of Shock Waves in Combustible Gaseous Mixture, Shock Waves. 10 (2000) 197–204.

[2] N.N. Smirnov, O.G. Penyazkov, K.L. Sevrouk, V.F. Nikitin, L.I. Stamov, V.V. Tyurenkova, Detonation Onset Following Shock Wave Focusing, Acta Astron. 135 (2017) 114–130.

[3] A.A. Vasil'ev, Cellular Structures of a Multifront Detonation Wave and Initiation (Review), Combust. Explos. Shock Waves. 51 (2015) 1–20.

[4] V.A. Levin, V.V. Markov, T.A. Zhuravskaya, S.F. Osinkin, Nonlinear Wave Processes That Occur during the Initiation and Propagation of Gaseous Detonation, Proc. Steklov Inst. Math. 251 (2005) 192–205.

[5] S.M. Frolov, Initiation of Strong Reactive Shocks and Detonation by Traveling Ignition Pulses, J. Loss. Prev. Proc. Ind. 19 (2006) 238–244.

[6] S.M. Frolov, I.V. Semenov, P.V. Komissarov, P.S. Utkin, V.V. Markov, Reduction of the Deflagration-to-Detonation Transition Distance and Time in a Tube with Regular Shaped Obstacles, Dokl. Phys. Chem. 415 (2007) 209–213.

[7] C. Hu, C.-W. Shu, Weighted Essentially Non-Oscillatory Schemes on Triangular Meshes, J. Comput. Phys. 150 (1999) 97–127.

[8] L.F. Figueira da Silva, J.L.F. Azevedo, H. Korzenowski, Unstructured Adaptive Grid Flow Simulations of Inert and Reactive Gas Mixtures, J. Comput. Phys. 160 (2000) 522–540.

[9] F. Togashi, R. Lohner, N. Tsuboi, Numerical Simulation of H2/Air Detonation using Unstructured Mesh, Shock Waves 19 (2009) 151–162.

[10] H. Shen, M. Parsani, The Role of Multidimensional Instabilities in Direct Initiation of Gaseous Detonations in Free Space, J. Fluid. Mech. 813 (2017) Paper R4.

[11] Hu G. A Numerical Study of 2D Detonation Waves with Adaptive Finite Volume Methods on Unstructured Grids, J. Comput. Phys. 331 (2017) P. 297 – 311.

[12] A.I. Lopato, P.S. Utkin, Numerical Study of Detonation Wave Propagation in the Variable Cross-Section Channel Using Unstructured Computational Grids, J. Combust. (2018) Article ID 3635797.

[13] O.V. Achasov, S.A. Labuda, O.G. Penyaz'kov, Initiation of Detonation by Gasdynamic Methods, J. Eng. Phys. Thermophys. 69 (1996) 807–813.

[14] E. Schultz, J. Shepherd, Validation of Detailed Reaction Mechanisms for Detonation Simulation, Report No. FM99-5, CalTech Explosion Dynamics Lab., 2000.

[15] O.G. Penyazkov, K.L. Sevruk, V.E. Tangirala, A.J. Dean, B. Varatharajan, Shock Wave Initiation of Detonations in Propane/Air Mixtures, Proc. 20th ICDERS, Paper 91, 2005.

[16] G. Strang, On the Construction and Comparison of Difference Schemes, SIAM J. Num. Analys. 5 (1968) 506–517.

[17] M.-S. Liou, C.J.Jr. Steffen, A New Flux Splitting Scheme, J. Comput. Phys. 107 (1993) 23–39.

[18] G. Chen, H. Tang, P. Zhang, Second-Order Accurate Godunov Scheme for Multicomponent Flows on Moving Triangular Meshes, J. Sci. Comput. 34 (2008) 64–86.

[19] I.V. Krassovskaya, M.K. Berezkina, Mechanism of Formation of Reflection Configurations over Concave Surfaces, Shock Waves 27 (2017) 431–439.